Average-Instantaneous, Unimodal and Multimodal Scattering Responses in Spatial Gaussian Channels

Konstantinos Mammasis, *Member, IEEE* Paolo Santi, *Member, IEEE,*

Abstract

In this paper the long standing problem of a heavy tailed power azimuth spectrum and the associated scattering mechanism that triggers its observance is undertaken using the geometry-based stochastic approach that was initially developed in [1], and is further extended herein. More specifically, the unimodal power azimuth spectrum (PAS) and joint power angular scattering response (PASR) are derived under the 2-D Gaussian scattering model. The developed methodology concentrates on two-dimensional (2-D) propagation and therefore provides theoretical insights for the azimuthal domain. At first, it is formally shown that a Gaussian scatter distribution in 2-D space gives rise to an angular power spectrum that may be well modeled by the Gaussian function; under the assumption of free space propagation. Numerical results are presented for higher path-loss exponents, where it is shown that heavier tailed functions such as the Lorentzian and Laplacian functions provide good fits to the derived spectrum. To complement earlier research works in this area, the geometry-based stochastic model developed in [1] is extended in order to express the instantaneous multimodal PASR, which significantly contributes to the estimated correlation statistics as shown in the paper. The 2-D spatial channel model developed herein, allows the distance from the observation point to vary, which enhances the validity of the derived PAS and PASR. Statistical results are provided for various distances from the observation point in order to facilitate any potential practical use of the derived 2-D model. Finally, an analytical expression for the correlation experienced between two antenna patterns is derived under the proposed model. The correlation function is expanded in a series of cylindrical harmonics and the correlation experienced is estimated, which reveals the impact of the instantaneous PASR and average PAS on the correlation function.

Index Terms

Angular power scatttering response, power angular spectrum, wireless spatial channel modeling, antenna arrays.

I. INTRODUCTION

COMMUNICATION architectures that employ multi-element antennas have gained considerable attention in the academic community in recent years. In particular, the considerable throughput capacity benefits potentially offered by these systems have increased interest in spatial channel modeling. In fact, spatial channel modeling is fundamental in estimating one of the key performance indicators in multi-element antennas, i.e., the correlation experienced between adjacent links which, in turn, depends on the response of each antennae in the array. Therefore, a full understanding of the physical mechanisms governing spatial correlation may help us to resolve some of today's intriguing tasks in antenna design and pattern diversity. Correlation is largely affected by the so-called angular power spectrum (APS),

Konstantinos Mammasis is a Researcher in the National Research Council of Italy, via Giuseppe Moruzzi 1, 56124, Pisa, Italy e-mail: konstantinos.mammasis@iit.cnr.it.

Paolo Santi is a Senior Researcher in the National Research Council of Italy, via Giuseppe Moruzzi 1, 56124, Pisa, Italy e-mail: paolo.santi@iit.cnr.it.

also known as power azimuth spectrum (PAS) in the two-dimensional (2-D) plane. The PAS has been extensively used for the estimation of channel statistics in various standardized spatial channel models, e.g., [2], [3]. In the 2-D case, the authors of [4] observed through experimental investigations that a Gaussian distribution in angle of arrival (AoA) gives rise to a Laplacian-like PAS. The Laplacian function was also considered in [5]. In general, many different shapes of AoA and APS have been proposed in the literature, considering different scatterer distributions such as Gaussian, von Mises and uniform [6], [7]. A related geometry-based approach was also proposed in [8] to cover both macro and micro types of cells. Among the fundamental works in this area is [9], where Fuhl *et al.* developed a modeling approach to estimate the spatial correlation coefficients for a variety of angular distributions. Modeling the dependency of the directional channel impulse response and the associated parameters is the primary objective in spatial channel modeling.

The main goal of this paper is to provide a theoretical framework for a *complete* (i.e., including PAS) 2-D spatial channel characterization under the Gaussian scatterer assumption and therefore complete the analysis already presented in [1]. The authors in [1] laid the foundations of the model extended herein, by jointly deriving distance and angular statistics, thus allowing a theoretical characterization of the expected PAS under the 2-D Gaussian model. The notions of PAS (a *time-averaged* estimation of the power spectrum at the receiver) and PASR (an estimation of the *instantaneous* power spectrum observed at the receiver) were first explained in [1], with particular emphasis given to the latter definition, i.e., PASR. While PASR characterization is important for the statistical analysis of a single channel impulse response (CIR) snapshot (provided adequate resolution in space-time), the time-averaged version obtained from the averaging of many CIR snapshots, i.e. PAS, is fundamental for estimating important performance parameters such as spatial correlation between antenna elements, link capacity, etc. Thus, a major goal of this paper is to provide a thorough characterization of the PAS under the 2-D spatial channel model introduced in [1], considering not only free-space propagation as done in [1], but also for higher path-loss exponents. A major finding of our analysis is that the expected PAS attains a Gaussian functional form for the free space exponent, while a heavier tailed function provides a more accurate fit for higher path-loss exponents. Therein, the Lorentzian function is an excellent candidate, but the Laplacian function performs very well too, thus providing a theoretical framework for explaining functional forms of the PAS observed in real-world measurements. The fits are assessed using the mean square error metric.

Another major contribution of this paper is the derivation of the PASR in presence of *multiple* scatterer

clusters in the propagation environment. This extension of the model is fundamental to improve its accuracy, since radio environments with multiple scatterer clusters are frequently observed in real world. An important feature of the derived multi-cluster model is that, differently from previous approaches, in the presented model the "weight" of a scatterer cluster is implicitly computed as a byproduct of the distance of the cluster from the transmitter and receiver station. To prove the practicality of this approach, we consider a simulation scenario with two scatterer clusters, and compute the observed PASR accordingly.

Finally, the analysis continues by estimating the spatial correlation experienced between adjacent antenna elements under the derived unimodal and multimodal power angular scattering responses, and extensive comparisons with other well-known angular power fields are presented. These comparisons indicate that existing models tend to over-estimate the correlation between the adjacent links, which may be attributed to the fact that other models such as Laplacian and von-Mises do not account for distance from/to transmitter and receiver station when computing the correlation statitistics. To achieve the above, the correlation function is derived as a result of the expansion of a plane wave into a series of cylindrical harmonics, which reveals the response of an antenna to the derived angular power scattering field.

The rest of this paper is organized as follows: in Section II the full derivation of the expected PAS experienced under the Gaussian model for various path-loss exponents is presented. Section III derives the angular power scattering response experienced at the observation point in space under the existence of multiple scatter clusters, giving rise to the multimodal PASR. In Section IV, the response of an antenna to the derived angular power field is assessed by correlating it to an adjacent antenna's response for the derived and other well-known angular power fields; essentially, serving as a *performance metric*. In the same section the field is expanded under a circular array topology from which various correlation matrices are obtained. Results are presented for the derived, Laplacian and von-Mises fields. Finally, Section V summarizes the main contributions of this work.

II. A Two-Dimensional Gaussian Power Angular Spectrum

In this section, the observed PAS under the Gaussian scattering mechanism is derived, which was not presented in [1]. Additionally, this work investigates the effect of higher path-loss exponents on the corresponding spectrum. The final result is therefore in a spectrum form and not a distribution function, that characterizes the average spatial channel statistics and not the instantaneous response (PASR). Hence, it is of interest to estimate the *expected* amount of power outgoing in an arbitrary direction ψ. In mathematical

terms the PAS is equivalent to:

$$\text{PAS} = E[f(\varrho_e|\psi)]f(\psi),$$

where ϱ_e defines the outgoing power along direction ψ, and $f(\varrho_e|\psi)$ denotes a conditional distribution. The above definition was also given in [4]. To derive the above, two random quantities need to be derived: the density of scatterers observed by Tx along direction ψ – i.e., the angular scatterer density $f(\psi)$–, and the density of power transmitted by Tx, outgoing to a scatterer along direction ψ – i.e., the scatterer power density $f(\varrho_e)$ (see Fig. 1). In [1], explicit expressions for the characterization of the radial and angular domain were provided, some of which will be re-stated here for convenience.

A. PAS Derivation under 2-D Gaussian Scattering

First, consider the transformation of the Gaussian distribution in polar co-ordinates and the resultant expression, which could be summarized as follows:

$$f_{R,\Psi}(\|\boldsymbol{\Omega}_{\rho_2,sc}\|,\psi) = \frac{\|\boldsymbol{\Omega}_{\rho_2,sc}\|}{2\pi\sigma^2}e^{-(\|\boldsymbol{\Omega}_{\rho_2,sc}\|^2+\|\boldsymbol{\Omega}_o\|^2)/2\sigma^2}e^{\|\boldsymbol{\Omega}_{\rho_2,sc}\|\|\boldsymbol{\Omega}_o\|\cos(\psi-\psi_o)/\sigma^2}. \tag{1}$$

In (1), $\|\boldsymbol{\Omega}_o\|$ denotes the distance of the mean directional vector $\boldsymbol{\Omega}_o$ to the scatter cluster (see Fig. 1) and ψ_o the associated azimuthal angle to this vector. This function represents the so-called distance-dependent AoA spectrum as observed at Tx $= \rho_2$. Under this representation, the density at ρ_2 is taken with respect to the center of gravity (x_o, y_o) of the scatterers in its vicinity. Note that Fig. 1 has been created in view of the multiple cluster scenario that is also of interest in this work. Consequently, the angular distribution $f(\psi)$ is obtained by integration of the joint distribution over the whole radial space:

$$\begin{aligned}
f(\psi; \|\boldsymbol{\Omega}_o\|, \sigma) &= \int_0^\infty f(\|\boldsymbol{\Omega}_{\rho_2,sc}\|,\psi)d\|\boldsymbol{\Omega}_{\rho_2,sc}\| \\
&= \frac{1}{4\pi}e^{-\|\boldsymbol{\Omega}_o\|^2\sin[\psi-\psi_o]^2/2\sigma^2}\left(2e^{-\|\boldsymbol{\Omega}_o\|^2\cos[\psi-\psi_o]^2/2\sigma^2}\right. \\
&\left. + \frac{1}{\sigma}\|\boldsymbol{\Omega}_o\|\sqrt{2\pi}\cos[\psi-\psi_o]\left(1+\text{Erf}\left[\frac{\|\boldsymbol{\Omega}_o\|\cos[\psi-\psi_o]}{\sqrt{2}\sigma}\right]\right)\right).
\end{aligned} \tag{2}$$

This is the general form of the distribution of angles for a Guassian distribution of scatterers in 2-D. The distribution of angles is a function of ψ. As shown in [1], increments in the length of $\boldsymbol{\Omega}_o$ cause an increase in the concentration of angles, which is in accordance with intuition, since by increasing the distance from the observation point the concentration of angles increases. The functional form of (2) can be found in [1].

Fig. 1 HERE

To proceed in estimating the PAS, the conditional distribution of distances on the angle ψ is obtained, which after normalization obtains the following form:

$$
\begin{aligned}
f(\|\mathbf{\Omega}_{\rho_2,sc}\| | \psi) &= \frac{f(\|\mathbf{\Omega}_{\rho_2,sc}\|, \psi)}{f(\psi)} \\
&= 2e^{\left(-\|\mathbf{\Omega}_{\rho_2,sc}\|^2 + 2\|\mathbf{\Omega}_{\rho_2,sc}\|\|\mathbf{\Omega}_o\| \cos[\psi - \psi_o]\right)/2\sigma^2} \|\mathbf{\Omega}_{\rho_2,sc}\|/D,
\end{aligned}
\tag{3}
$$

$$
D = 2\sigma^2 + e^{\|\mathbf{\Omega}_o\|^2 \cos[\psi-\psi_o]^2/2\sigma^2} \|\mathbf{\Omega}_o\| \sigma\sqrt{2\pi} \cos[\psi - \psi_o] \left(1 + \text{Erf}\left[\frac{\|\mathbf{\Omega}_o\| \cos[\psi - \psi_o]}{\sqrt{2}\sigma}\right]\right).
$$

The derived density, defining distance density conditioned on an infinitesimal angular sector, closely resembles the derived distribution of distances in terms of functionality [1]; with the dependency being shifted to the angular domain. The derived distribution is two-fold; it obtains a symmetric or asymmetric to the mean shape within an angular sector $\Delta\psi$ depending on the characteristics of the mean direction vector, i.e. the angle ψ_o, and length of $\mathbf{\Omega}_o$. The distribution is symmetric provided that conditioning on angle ψ occurs within the angular sector $\Delta\psi$.

In the following, the conditional distribution of distances is transformed into a power distribution according to the free-space propagation model. Subsequently, the expectation of each conditional distribution is obtained and as shown a Gaussian-like angular power spectrum emerges. To proceed, the conditional distribution of distances near the mobile ρ_2 is assumed to be $f(\|\mathbf{\Omega}_{\rho_2,sc}\| | \psi)$ with a small $\|\mathbf{\Omega}_o\|/\sigma$ ratio, which is representative of a macrocellular scenario with the scatterers being relatively close to the receiver as opposed to the transmitter. A hypothetical transmitter is placed in another point on the Euclidean plane. The length of the mean distance vector $\mathbf{\Omega}_c \gg \mathbf{\Omega}_o$. As shown in [1] the power extracted at the scatter cluster may be well described by an Inverse-Gamma distribution, which makes the presented analysis more tractable. To proceed, consider the following transformation function:

$$
\varrho_e = \alpha/\|\mathbf{\Omega}_{\rho_2,sc}\|^2,
\tag{4}
$$

where α typically accounts for the transmit power, antenna gain and the cluster's cross sectional area. We denote $w = \|\mathbf{\Omega}_{\rho_2,sc}\|$ for notational convenience. Subsequently, transforming the conditional distance distribution into a power conditional distribution, we re-write (4) as follows:

$$
\varrho_e = \frac{\alpha}{w^2} \Rightarrow w = \sqrt{\frac{\alpha}{\varrho_e}},
\tag{5}
$$

whose derivative with respect to the variable ϱ_e is given by

$$
\frac{dw}{d\varrho_e} = -\frac{\sqrt{\alpha}}{2\varrho_e\sqrt{\varrho_e}}.
\tag{6}
$$

After substitution of (5) into (3) and making use of the above derivative, the conditional distribution of power in each angle obtains the following form:

$$f(\varrho_e|\psi) = \alpha e^{\left(-\alpha/\varrho_e + 2\sqrt{\alpha/\varrho_e}\|\mathbf{\Omega}_o\|\cos[\psi-\psi_o]\right)/2\sigma^2}/\varrho_e^2 D,$$

$$D = 2\sigma^2 + e^{\|\mathbf{\Omega}_o\|^2 \cos[\psi-\psi_o]^2/2\sigma^2}\|\mathbf{\Omega}_o\|\sigma\sqrt{2\pi}\cos[\psi-\psi_o]\left(1 + \mathrm{Erf}\left[\frac{\|\mathbf{\Omega}_o\|\cos[\psi-\psi_o]}{\sqrt{2}\sigma}\right]\right). \tag{7}$$

In Fig. 2 the derived distribution is examined under the conditional case of angles $\psi = 180°$ and $\psi = 230°$ respectively. The cluster is centered at $\psi_o = 180°$, at a mean distance of $\|\mathbf{\Omega}_o\| = 10$ and $\sigma = 3$.

Fig. 2 HERE

The derivations thus far are based on the fundamental inverse square law assumption, which is only valid in the far-field of the antenna response. The distance variable $r \in [0, \infty)$ and the corresponding transformation function introduces an ambiguity into the derived spectrum. This ambiguity originates from the fact that ϱ_e will be similarly defined, $\varrho_e \in [0, \infty)$, if left unchanged. However, the power extracted at the scatter cluster and subsequently received by the receiver cannot exceed the power at the boundary of the far-field zone P_f. Therefore, instead of defining the conditional random variable $P_e|\psi$ within $0 \leq P_e|\psi < \infty$, it should be defined as $0 \leq P_e|\psi \leq P_f$. To introduce this dependency into the model there are two methodologies that could be followed: *i)* posing a restriction to the distance variable r by left-truncating the joint density function in (1), or *ii)* transform (7) such that the conditional distribution of power on angle is truncated from the right, i.e. $0 \leq P_e|\psi \leq P_f$. The first case is equivalent to creating a circular region in space, inside which the probability of finding a scatterer is zero and resultantly the distance variable can only be defined outside this circular region, whose minimum distance is dictated by $r_{min} = 2D^2/\lambda$ (Fraunhofer region), with D being the antenna dimension and λ the wavelength of radiation. The truncated density can then be obtained by computing $(1 - F(r_{min}))$–where $F(r_{min})$ denotes the cumulative distribution function– and by dividing this probability by the original joint density $f(r, \psi)$. Alternatively, one is forced to use the second method proposed herein, under which the truncated conditional power density takes the following form:

$$f_{tr}(\varrho_e|\psi; P_e \leq P_f) = f(\varrho_e|\psi)/F(P_f),$$

$$F(P_f) = \int_0^{P_f} f(\varrho_e|\psi)d\varrho_e. \tag{8}$$

Not only this definition is more intuitive, but it also assists in finding the appropriate limits when evaluating the expectation of the truncated random variable shown in (9). Essentially, this definition accounts for

far-field scattering and bounds the average PAS above P_f. It follows directly from (7) and (8) that the 2-D PAS is Gaussian-like, having considered the expectation of the truncated conditional variable in (8):

$$\text{PAS} = f(\psi)E\left[P_e|\psi\right] = f(\psi)\int_0^{P_f} \varrho_e f_{tr}(\varrho_e|\psi)d\varrho_e, \qquad 0 \leq P_e \leq P_f. \tag{9}$$

The expected power in each direction has been scaled by the probability density of finding a scatterer along the conditioning angle. Therefore, the final spectrum form is actually a weighted angular function. As discussed, the expected power in each direction is upper bounded by the power $P_f = \alpha/r_{min}^2$ at the boundary of the far-field zone. In view of the above, it should be highly emphasized that a more general model, accounting for the near-field dependencies and associated impact on the average PAS would be an important contribution, especially, considering that the impact of near-field correlation has not received a full treatment in the literature. Under the proposed approach, the ratio $\|\mathbf{\Omega}_o\|/\sigma$ is assumed to be larger than r_{min}, in order to obey the far-field dependence. Note that the resultant spectrum may also be truncated due to the limited angular range of incoming paths, as well as the associated radial characteristics. Truncated spectrum forms have been observed in practice that may be typically attributed to the directionality of the antenna pattern. The evaluation of the above expectation for each conditional distribution in the range $[0, 2\pi)$ and the corresponding multiplication by the angular density is shown in Fig. 3; superimposed with the evaluation of higher pathloss exponents. For clarity the y-axis has been logarithmically scaled. Note that the above integral was evaluated numerically[1]. Through a statistical goodness-of-fit assessment it was revealed that a Gaussian function approximates well the derived PAS in free space conditions. The Gaussian PAS was also proposed in [10]. Additionally, the PAS estimated from measurements in Stockholm and Aarhus in [11] may serve as another indication of a Gaussian PAS observed in practice.

Fig. 3

To complete the analysis presented herein, the derived transmitting PAS is evaluated under different path-loss exponents. The transformation function is modified accordingly, $\varrho_e = \alpha/\|\mathbf{\Omega}_{\rho_2,sc}\|^n$, where n is the path-loss exponent. As shown in Fig. 3 increasing the path-loss exponent results in a loss of power in the corresponding angle. This observation follows theoretical intuition, since at higher path-loss exponents the expected power on each angle should drop in order to compensate for the higher loss encountered in the propagation path. The effect of path-loss variations on the power angular spectrum is one of the major

---

[1]Alternatively, an analytical expression may be obtained by approximating (7) with an Inverse-Gamma distribution, whose first order moment is given by $E\left[P_e|\psi\right] = \beta/\alpha - 1$. Mapping the associated expectation in the range $0 \leq \psi < 2\pi$ reveals a Gaussian-like PAS.

findings of this work, since as shown in Fig. 3 and Fig. 4 the spectrum attains heavier tails, as n increases. Among various examined functions, the three-parameter Lorentzian[2] function performed extremelly well in capturing the derived spectrum's sharp peak characteristics. Note that the above analysis complements the analysis presented in [1], where emphasis was placed on the instantaneous power angular scattering response, i.e. the probability of observing exactly power ϱ_e at an incoming angle ψ, at a generic instant of time t. In addition to [1], this paper provides an exact derivation of the PAS due to Gaussian scattering, providing a thorough analysis of this important subject and for the first time a complete theoretical framework under which a heavier tailed spectrum, e.g. Laplacian spectrum, is observed.

<center>Fig. 4 HERE</center>

Please refer to [4] for the measurement-based approach, where the authors obtained a Laplacian PAS from a Gaussian distribution in angle of arrival. As shown in Fig. 4 however, although the Laplacian function serves as a good candidate, the Lorentzian function provides a better fit. The mean square error (MSE) metric was used as a goodness-of-fit indicator, which confirmed that the Lorentzian fit is superior for all path-loss exponents $n > 2$.

B. Transforming the Transmitting PAS into a Receiving PAS

Converting the transmitting PAS into the receiving PAS necessitates the use of a transformation function, similar to the one used in [1]. In essence, (9) needs to be modified so that it accounts for the mapping of power $\varrho_r|\varphi, \psi$, so that it express the bi-directional nature of the spectrum. Bi-directionality imposes a dependency between the transmitting PAS and receiving PAS, independently of whether the study focuses on the *average* or *instantaneous* form of the spectrum. Thus, we are interested in the modification of the *average* PAS at the RX-MS due to transmission from the TX-BS. The final transformation function considering the transmission from TX-BS to the scatter cluster in angle ψ and the associated loss of power along the incoming scattered direction φ is also a function of the distance between the scatter cluster and the RX-MS. The transformation function due to the derived spectrum form is akin to the transformation function proposed in [1], equation (10) therein, accounting for the conditional distributions in this instance, i.e., (7). Its form is equivalent to: $P_r|\varphi = P_e|\psi (1/Y|\varphi)$. $P_e|\psi$ denotes the extracted power at the scatter cluster in ψ due to transmission from TX-BS. The product of the two random variables – i.e., the random variable from the distribution in (7) and the transformed random variable $1/Y|\varphi$ that

---

[2]The Lorentzian function, also known as Cauchy function, is typically defined as: $f(\varrho) = \alpha/((\varrho - \gamma)^2 + \delta)$, where α, γ and δ are the parameters of the distribution.

is also distributed[3] as (7), however with different parameters–results in the desired conditional random variable, which cannot be obtained in an analytical form, unless an approximation is performed in (7) with possibly other well-known functions. As mentioned in Section II, a good approximation to (7) is achieved using the Inverse-Gamma distribution, whose application in this instance leads to a closed-form solution for the PAS (and PASR as we will shortly see). In this respect, we can trivially arrive at $E\left[P_r|\varphi\right]$, which as expected will be a scaled version of $E\left[P_e|\psi\right]$; we recall that the product of two Inverse-Gamma random variables results in another Inverse-Gamma random variable [1].

III. Unimodal and Multimodal Power Angular Scattering Responses under Spatially Gaussian Channels

In this section, the instantaneous power angular scattering response is highlighted and used in order to extend the derived model into the multi-cluster case. The reason of shifting our current focus to instantaneous power angular scattering response rests on its simplicity in studying multimodal scenarios. The power angular scattering response is the result of multiplication between the conditional distribution of power in each angle, i.e. (7), and the distribution of angles given in (2). In this respect, we are able to study correlation due to the fluctuating instantaneous PAS–named *power angular scattering response*–and not only the average PAS. In the following, the power angular scattering response is extended to multiple scatter clusters and any uncovered statistical dependencies in [1] – between the parameters of the various distributions – are addressed, at least for the unimodal case.

A. Unimodal Power Angular Scattering Response Formulation

To proceed, first consider the unimodal response resulting from the combination of (2) and (7):

$$f(\varrho_e, \psi) = f(\varrho_e|\psi) \times f(\psi; \|\mathbf{\Omega}_o\|, \sigma) = \frac{1}{4\pi \varrho_e^2 \sigma^2} e^{-\left(1 + \|\mathbf{\Omega}_o\|^2 \varrho_e - 2\|\mathbf{\Omega}_o\|\sqrt{\varrho_e}\cos[\psi - \psi_o]\right)/2\varrho_e\sigma^2}. \tag{10}$$

The derived distribution jointly accounting for extracted power ϱ_e along direction ψ denotes the transmitting power angular scattering response, and needs to be transformed depending on the side of the link where the received spectrum is to be observed. Bi-directionality imposes a dependency between the transmitting PASR and receiving PASR, as is the case for the transmitting and receiving PAS. Similarly, we are interested in the modification of the *instantaneous* PASR due to transmission from the BS-TX. Thus, although (10) provides us with an analytical expression of the joint distribution in power and

---

[3]The validity of this statement is clarified here for convenience. The random variable Y denotes the new set of squared distances from the RX-MS to the scatter cluster, $\|\mathbf{\Omega}_{\rho_1,sc}\|^2$. To arrive at this distribution, (3) needs to be transformed accordingly, and this transformation is exactly the same as the one followed earlier for obtaining $f(\varrho_e|\varphi)$.

angular dimensions (the desired power angular scattering response), it needs to be modified so that it accounts for the mapping of power $\varrho_r|\varphi, \psi$, in order to express the bi-directional nature of the channel. The transformation procedure is similar to the one detailed earlier in the closing paragraph of Section II, and leads directly to $f(\varrho_r, \phi)$. In this respect, we can trivially arrive at $f(\varrho_r, \phi)$, which as expected will be a scaled version of $f(\varrho_e, \psi)$. As shown in [1], the product of two Inverse-Gamma random variables results in a random variable that is also distributed as Inverse-Gamma. The evaluation of (10) for the exemplary case of $\|\mathbf{\Omega}_o\| = 10$, $\sigma = 3$ and $\psi_o = 180^o$ appears in Fig. 5.

Figure 5 HERE

To simplify the derivations and present a more tractable methodology for obtaining the PAS and PASR at the TX-BS, the authors in [1] instead of dealing with the conditional distributions, directly tranform distances into power values and finally express the joint distribution of power and angle as a product of two marginal distributions, i.e., the power density $f(\varrho_e)$ and the angular density $f(\varphi; \|\mathbf{\Omega}_o\|, \sigma)$ that was derived earlier. This methodology introduces an error in the approximation of the original joint function, however as shown in Section III-A1, this error diminishes to zero under certain parameter settings. Accordingly, the unimodal response was given as:

$$f(\varrho_e, \varphi) = f(\varrho_e) \times f(\varphi; \|\mathbf{\Omega}_o\|, \sigma). \tag{11}$$

In turn, the power density $f(\varrho_e)$ is well approximated with an Inverse Gamma distribution $\sim (\alpha, \beta)$ as shown in [1]. It is then trivial to transform P_e to P_r, which as shown in [1], it is a random variable also distributed as Inverse-Gamma. Direct substitution in (11) and alternation of the parameters of the angular density as viewed by the TX-BS leads to the receiving power angular scattering response.

1) Mutual Information: The validity of the independence assumption used in (11) is confirmed by examining the Kullback–Leibler divergence between the actual joint distribution and the product of marginals, which at least classifies the circumstances under which independence can be claimed. This is formally denoted as the Mutual Information (MI) and is a measure of distance between two density functions or can also be understood as the degree of correlation between them. The MI is attained by taking the relative entropy of the actual joint distribution with respect to the distribution of the product of marginals [12]:

$$I(P_e, \Psi) = \iint\limits_{\varrho_e, \psi} f(\varrho_e, \psi) \log_e(\frac{f(\varrho_e, \psi)}{f(\varrho_e)f(\psi)}) d\varrho_e d\psi. \tag{12}$$

It was observed that for large values of $\|\mathbf{\Omega}_o\|$ the product of marginals serves as a good approximation. As found experimentally, this approximation always holds given that the length of the mean directional vector $\mathbf{\Omega}_o > 4\sigma$, where the mutual information reduced practically to zero for every case examined.

B. Multimodal Power Angular Scattering Response Formulation

Several research studies have indicated that the channel tends to cluster the directional components in space and time. The existence of multiple scatter clusters has been confirmed in the literature [2], [13]–[15]. Procedures for estimating the parameters of various clusters identified in measurements can be found in [16], [17], among others. To extend the unimodal PASR into a multimodal PASR it suffices to represent the spatial domain structure in an additive manner, i.e., summation of the scatter clusters, the number of which is clearly dependent on the propagation environment, on the methodology used to identify them (clustering approach), and on various other criteria that fall beyond the scope of this work. The multimodal representation of the sum function (analogous to the mixture density function) $g(\varrho_r, \varphi)$ may be written in the following form:

$$g(\varrho_r, \varphi) = \sum_{n=1}^{N} f_n(\varrho_r) \times f_n(\varphi; \|\mathbf{\Omega}_o\|, \sigma), \tag{13}$$

where the ratio $\|\mathbf{\Omega}_o\|/\sigma$ is allowed to vary depending on the distance of each cluster to the observation point. Typically, each component's contribution in the mixture density is characterized by an associated prior weight. The membership contribution in clustering terms is determined by the power emanated from each cluster. In contrast, this is directly specified in the model derived in this work, since the power of each path is directly accounted for. To exemplify this, consider the case depicted in Fig. 1, where two spatial clusters appear. Our objective is to obtain the multimodal PASR at the MS: *i)* from the power extracted at each scatter cluster due to transmission from TX-BS *ii)* and re-emanated towards the RX-MS, albeit dictated by a new set of distances. Assume momentarily that lengths ρ_1 and ρ_1' are equivalent, which translates to the scatter clusters being equi-distant from the TX-BS and RX-MS. This fact does not necessitate the existence of equally weighted lobes in the multimodal density function, since the power extracted at each cluster may be due to different distances between them and the TX-BS. The assumptions made for simulating the above scennario are listed below:

1) The length of vector $\mathbf{\Omega}_o = \mathbf{\Omega}_o' = 5$.

2) The length of vector $\mathbf{\Omega}_c = 10$ and $\mathbf{\Omega}_c' = 16$.

3) The standard deviation $\sigma = 3$ for both clusters.

4) Free-space propagation $n = 2$.

It follows directly from the pre-stated assumptions and Table I that the estimated parameters for the transmitting side are: $\alpha_c = 3.7346, \beta_c = 0.0311$ for the cluster at a mean distance of $\|\mathbf{\Omega}_c\| = 10$, and $\alpha_{c'} = 7.7332, \beta_{c'} = 0.0281$ for the cluster at $\|\mathbf{\Omega}_c\| = 16$. On the other side, the estimated parameters are $\alpha_o = \alpha_{o'} = 1.5887, \beta_o = \beta_{o'} = 0.0358$. After considering the analysis in [1]–more specifically formulae (13) detailed therein–the estimated parameters that characterize the power density function at the TX-BS (as a result of re-transmission from the scatter cluster) for each pair of clusters are: $\alpha_{o_1} = 0.95$, $\beta_{o_1} = 0.0002$ and $\alpha_{o'_1} = 1.2$, $\beta_{o'_1} = 0.0001$ respectively. The resultant mixture density appears in Fig. 6. Note that the proposed modeling approach captures the effect of increased distance due to the second cluster, i.e. $\mathbf{\Omega}'_c = 16$, and reflects it on the PASR by assigning a lower power weight on the second lobe at $\varphi_o = 180°$. In the next section, an application of the derived unimodal and multimodal fields is provided. The fields are assumed to be impining on an antenna array of a circular topology, aiming at the assessement of the spatial correlation between the patterns.

Fig. 6 HERE

1) Characterizing the Inverse Gamma Distribution: To characterize various cases and facilitate the modeling process, a statistical analysis has been performed for the approximation of the Inverse-Gamma distribution in all instances encountered under the assumption of independence. The estimated parameters presented below correspond to various mean distances from the observation point. In order to derive the parameters of the receiving PASR $f(\varrho_r, \varphi)$, it is essential to first obtain the parameters of the transmitting power density function $f(\varrho_e)$. To achieve this, equation (10) in [1] needs to be considered and any desirable pair of $\|\mathbf{\Omega}_o\|, \|\mathbf{\Omega}_c\|$ specified apriori. A rejection sampling technique was used to sample from the derived power density function and a maximum likelihood estimation procedure followed in order to estimate and assess the fit of the Inverse Gamma distribution to the drawn sample. The estimated parameter values can then be inserted into equation (13) in [1] to obtain the receiving PASR parameter values. This is exactly the procedure followed to estimate the parameters for the two cluster scenario analyzed ealier. For a detailed analysis the reader is referred to [1]. Herein, the addition of Table I serves as an assisting tool for the simulation of a wide range of scenarios of the derived model. Finally, all derived distributions and associated approximations (where applicable) are listed in Table II.

Table I,II HERE

IV. AN APPLICATION: SPATIAL CORRELATION STATISTICS

A potential application of the derived model is for the assessement of spatial correlation in antenna patterns. In essence, the derived field may be used to assess the responses of two adjacent antenna elements, due to the derived angular power field impinging on them. The antenna response of a radiating element is dependent on various factors, which cannot all be accounted for in this work. For instance, the mounting platform, mutual coupling between the radiating elements, individual radiation patterns (embedded), power angular field and associated directions in space, as well as, polarization properties are among the main contributing factors. The associated complexity in analyzing such systems has always been deterring from a modeling perspective. To simplify the analysis and concentrate on the main targets of this work, let us assume that there exist a circular topology of elements that possesses omnidirectional (2-D) properties. The question that naturally arises is the following: "*How does the antenna response due to an impinging power angular field $f(\varrho_r, \varphi)$ at element r_1 differs from the antenna response at an adjacent element r_2 due to the same power angular field?*".

In the literature, research works attempting to provide an insight of the spatial correlation estimation [17], [18] have mostly assumed normalized power angular fields, i.e., power angular fields originating from distributions that are strictly defined on the circle or the sphere, e.g., von-Mises or von-Mises Fisher. Thus, the above assumption explicitly states that each incoming plane wave is of unit amplitude. Admittedly, this is a questionable statement, since the restriction of the angular power field on the circular circumference or the surface of the sphere essentially removes the power dimension from the whole approach and conditions the power angular response to a particular distance, which is at least inaccurate from a geometry-based stochastic modeling perspective. Additionally, the array response is dependent on the amplitude/power of each incoming plane wave. It is therefore expected that the strength of each plane wave scales equally all harmonics in the wavefield decomposition process, and this should be considered.

A. Spatial Correlation Function

The analysis of the antenna response directly accounts for the normal Fourier tranform in 2-D. This basis function represents a plane wave that is expandable in a series of cylindrical functions, namely the *circular harmonics*. As expected, a series of plane waves impinge on the array with a power ϱ_r and from an angular direction φ_k. All plane wave contributions on the array's aperture are then weighted and integrated to yield the pattern-weighted response. A graphical representation of the above scenario is illustrated in Fig. 7. Note that the array is mounted on a cylindrical platform.

Fig. 7 HERE

The decomposition of a plane wave into circular harmonics on a circular aperture of radius $R = r$ can then be expressed by the following series:

$$e^{i\boldsymbol{k}^T \boldsymbol{r}} = e^{ikr\cos(\varphi_r - \varphi_k)} = \sum_{n=-\infty}^{\infty} i^n J_n(kr) e^{in(\varphi_r - \varphi_k)}, \tag{14}$$

where $J_n(\cdot)$ denotes the Bessel function of order n. In (14), k is the wavevector of the incoming planewave with $k = \|k\| = 2\pi f/c$, where f denotes the frequency of the planewave and r is the position of the observation point. The above equation is also known as the Jacobi-Anger expansion. More specifically, in polar coordinates the individular vectors are:

$$\boldsymbol{k} = k \begin{bmatrix} \cos \varphi_k \\ \sin \varphi_k \end{bmatrix}, \text{ and } \boldsymbol{r} = r \begin{bmatrix} \cos \varphi_r \\ \sin \varphi_r \end{bmatrix}. \tag{15}$$

The inner product of the two vectors is given by:

$$\boldsymbol{k}^T \boldsymbol{r} = kr\left[\cos\left(\varphi_r - \varphi_k\right)\right]. \tag{16}$$

The spatial correlation function (SCF) experienced between any two antenna responses can then be estimated using the following formulae, which serves as an extension of the SCF derived in [19]:

$$\rho(\boldsymbol{r}_1, \boldsymbol{r}_2) \equiv \rho(\boldsymbol{r}_2 - \boldsymbol{r}_1) = \int_0^\infty \int_0^{2\pi} f(\varrho_r, \varphi) e^{i(\boldsymbol{r}_2 - \boldsymbol{r}_1)\cdot \boldsymbol{k}} \varrho_r d\varphi_k d\varrho_r. \tag{17}$$

Combining (14) and (17) results in an analytical expression for the level of correlation between the two antenna responses:

$$\begin{aligned} \rho(\boldsymbol{r}_2 - \boldsymbol{r}_1) &= \int_0^\infty \int_0^{2\pi} f(\varrho_r, \varphi_k) \sum_{n=-\infty}^{\infty} i^n J_n(k\|\boldsymbol{r}_2 - \boldsymbol{r}_1\|) e^{in\varphi\|\boldsymbol{r}_2 - \boldsymbol{r}_1\|} e^{-in\varphi_k} \varrho_r d\varphi_k d\varrho_r \\ &= \sum_{n=-\infty}^{\infty} i^n J_n(k\|\boldsymbol{r}_2 - \boldsymbol{r}_1\|) e^{in\varphi\|\boldsymbol{r}_2 - \boldsymbol{r}_1\|} \int_0^\infty \int_0^{2\pi} f(\varrho_r) f(\varphi_k) e^{-in\varphi_k} \varrho_r d\varphi_k d\varrho_r \\ &= \sum_{n=-\infty}^{\infty} i^n \delta_n(\varrho_r) J_n(k\|\boldsymbol{r}_2 - \boldsymbol{r}_1\|) e^{in\varphi\|\boldsymbol{r}_2 - \boldsymbol{r}_1\|}. \end{aligned} \tag{18}$$

The coefficients of the power angular scattering response, i.e. $\delta_n(\varrho_r)$, may be obtained analytically by partioning the marginal densities and solving the two integrals independently. However, as explained in Appendix VII, the derived analytical expression is only a valid approximation for the case of $\|\boldsymbol{\Omega}_o\| \geq 2\sigma$. In case $\|\boldsymbol{\Omega}_o\| < 2\sigma$, the coefficients need to be computed numerically[4]. To validate the derived formulae,

---

[4]It was observed that although the angular density in (2) cannot be well-approximated by the von-Mises distribution for the $\|\boldsymbol{\Omega}_o\| < 2\sigma$ case, the associated contribution to the spatial correlation estimates was minor.

i.e. (27) in Appendix VII, the coefficients were also evaluated numerically. The coefficients derived in Appendix VII are therefore relevant only for the $\|\mathbf{\Omega}_o\| \geq 2\sigma$ case. Initially, a unimodal cluster case is examined, under which the corresponding coefficents are computed and compared with the coefficients of other well-known fields. An excellent fit between the numerical and the derived coefficients was observed. Note that the standard deviation of the von-Mises model was computed in accordance with the derived definition in Appendix VII and for the Laplacian distribution the definition in [19] was adopted. The concentration parameter of the von-Mises distribution was estimated using the length of the mean direction vector $\mathbf{\Omega}_o$, as: $\kappa = \|\mathbf{\Omega}_o\|^2/\sigma^2$ (see derivation in Appendix VII). The comparisons presented in the following not only present a useful insight on the discrepancies between the derived and the other models (e.g. Jakes, von-Mises), but also show the 2-D model's performance with respect to the *modified* von-Mises power angular field. The radial dimension is suppressed in the classic von-Mises representation. However, in Appendix VI a definition is provided that translates the angular spread of the von-Mises distribution so that it becomes representative of the distance at which the cluster is observed. We encourage the adoption of the presented von-Mises functional form, since it is more intuitive and at least captures some of the interesting spatial properties for clustered types of channels.

B. Pattern Correlation Dependency on 2-D Power Angular Scattering Response

In the following, an evaluation of the derived correlation function in (18) is performed under the assumed circular array topology employed at the receiving end for all pre-discussed power angular fields. In Fig. 8, the derived model is assessed for different lengths of the mean direction vector $\mathbf{\Omega}_o$, and as shown increasing this length increases spatial correlation; attributed to the increased concentration of incoming power in a smaller angular sector. Note also the Bessel oscillatory behavior of the correlation function as the length of $\mathbf{\Omega}_o$ tends to zero. The preceding point serves as another validation of the derived 2-D model, since at short lengths of the mean directional vector, the observation point is attracted to the centre of mass of the scatter points; indicating a full angular span. This follows Jakes model (also plotted in Fig. 8), in accordance to which, narrowband spatial correlation varies with frequency as a Bessel function, given the inter-element spacing, as expressed through: $J_0\left(k(\mathbf{r}_2 - \mathbf{r}_1)\right)$ [20]. As shown, there is an excellent agreement between the two models. In the same figure the von-Mises model is also presented, allowing a fair comparison only when conditioned at a particular distance $\|\mathbf{\Omega}_o\|$ (see Appendix VI). Of course, the shortfall of the von-Mises model lies in its inability to explicitly relate distance to angular concentration, in addition to the exclusion of power as a dimension. The relationship between distance and angular concentration is

only handled implicity through parameter κ. As shown, the derived model may be well approximated by the von-Mises density function when the concentration parameter is set *appropriately* (see Appendix VI). To exemplify this, consider the case where the length of the mean directional vector is set to ten (Fig. 8) and the corresponding estimate of the von-Mises field under the derived parameter, i.e. $\kappa = \|\mathbf{\Omega}_o\|^2/\sigma^2$. The goodness-of-fit is excellent. As depicted in the same figure, the correlation experienced under the two cluster model (recall discussion at Section III) drops–confirming intuition–since the addition of spatial clusters should de-correlate channel statistics. Rich multipath propagation decreases the spatial correlation by spreading the signal such that multipath components are received from different directions in space. Increasing the number of spatial clusters to five clearly shows this de-correlation tendency, which further validates the model's practicality.

Fig. 8 HERE

C. Pattern Correlation Dependency on 2-D Power Angular Spectrum

In Section IV-A the correlation due to the derived 2-D PASR was evaluated, indicating that a good approximation is provided by the von-Mises model under appropriate parameter settings. Although there are numerous evaluations of the correlation function in the literature, the impact of a more general model–accounting for the expected power on angle–has not been thoroughly analyzed, since a theoretical characterization of the expected power conditioned on angle poses more difficulties in contrast to the simple alternative of a probability density in the angular domain. Thus, the experienced correlation is subject to investigating the instantaneous spatial statistics (PASR) or the average spatial channel statistics (PAS). Both definitions have been widely used for simulating the SCF. Recall the analysis in Section II, where definiton (9) expresses the expected power conditioned on angle φ. Direct use of (9) in (18) transforms the latter into:

$$\rho\left(\mathbf{r}_2 - \mathbf{r}_1\right) = \sum_{n=-\infty}^{\infty} i^n J_n\left(k\|\mathbf{r}_2 - \mathbf{r}_1\|\right) e^{in\varphi_{\|\mathbf{r}_2-\mathbf{r}_1\|}} \int_0^{2\pi} \underbrace{\int_0^{\infty} \varrho_r f(\varrho_r|\varphi)d\varrho_r}_{\text{Conditional Expectation}} f(\varphi)e^{-in\varphi_k}d\varphi_k$$

$$= \sum_{n=-\infty}^{\infty} i^n \delta_{n,E} J_n\left(k\|\mathbf{r}_2 - \mathbf{r}_1\|\right) e^{in\varphi_{\|\mathbf{r}_2-\mathbf{r}_1\|}}. \tag{19}$$

Numerically evaluating (19) results in Fig. 9, which clearly illustrates the difference between the instantaneous PASR and average PAS on the behavior of the correlation function. For comparison purposes, the PAS's contribution to correlation is compared with the von-Mises model used earlier. The von-Mises model in this instance does not follow the correlation function estimated using the *expected* PAS. This

reveals the difference between the power-angular model (based on the expectation of power in angle) that is developed in this work and other unscaled angle of arrival models, in evaluating spatial correlation. High fidelity models such as the one developed herein, indicate that the performance of the average PAS significantly deviates from the probabilistic PASR approach, which seems to be very well approximated by known probability density functions such as the von-Mises, under appropriate parameter settings.

To accurately exploit the spatial correlation properties polarization should be included in the model. As this contribution highly focuses on the derivations on a geometry-based stochastic model, it would be difficult to also include a polarization assessement. A good treatment is provided in [21], and can trivially be replicated for the power angular fields developed in this work.

Fig. 9 HERE

V. Work Summary

In this paper, a spatial channel model has been developed under which it is formally shown that a Gaussian distribution of scatterers can justify both Gaussian, as well as, heavy-tailed (Lorentzian, Laplacian) functional forms of the PAS, depending on the path-loss exponent. The presented spatial channel model completes the initiatory work in [1], which has now been extended in order to account for the average incoming power from each direction due to the presence of a Gaussian-scatter cluster in space. The model was enhanced so to account for various path-loss exponents and therefore generalize the proposed methodology. The average PAS was fully derived and as shown it attains a Gaussian shape for the free space exponent, while the spectrum tends to Lorentzian as the exponent increases. Notably the Laplacian function provided a very good fit to the derived spectrum, validating earlier measurement-based findings in the literature that claim the observance of a Laplacian power angular spectrum due to Gaussian scattering in the angular domain. Further, it was shown how the model can be extended to account for multiple scatterer clusters, with the flexible property that the "weights" used to balance the contribution of the various clusters to the observed PAS are directly derived from the reference geometry. Finally, various contributions in terms of the spatial correlation experienced between adjacent antennas were made, especially concerning the derivations of the coefficients for the derived power angular field. As shown earlier, the average PAS statistics significantly differ from the instantaneous PASR in terms of the experienced correlation. The derived PASR can always be well-approximated by other probabilistic models such as the von-Mises model under appropriate parameter settings. To assist the reader and allow a fair

comparison between the PASR and the von-Mises model, an exact relationship between the concentration parameter of the von-Mises distribution and the model parameters was derived.

The model presented in this paper can prove extremely useful in improving accuracy of MIMO channel performance parameter estimation, especially in those settings where co-existence of several spatially separated MIMO links is considered. To this purpose, we believe a major avenue for future work is complementing the proposed model with techniques aimed at estimating MIMO link channel capacity as a function of the scatterer geometry. The above is a challenging task considering that the authors have introduced a dependency between the transmitting and receiving power angular spectrums.

VI. APPENDIX: DERIVING THE VON-MISES CONCENTRATION CONSTANT

The von-Mises distribution is a well-known directional distribution suitable for the statistical description of directional variables. It is obtained by conditioning the Normal distribution on the circle. As shown in [1], the joint density function in polar co-ordinates after transformation of the corresponding Gaussian density in Cartesian co-ordinates takes the following form:

$$f_{R,\Phi}(\|\mathbf{\Omega}_r\|, \varphi) = \frac{\|\mathbf{\Omega}_r\|}{2\pi\sigma^2} e^{-(\|\mathbf{\Omega}_r\|^2 + \|\mathbf{\Omega}_o\|^2)/2\sigma^2} e^{\|\mathbf{\Omega}_r\|\|\mathbf{\Omega}_o\|\cos(\varphi-\varphi_o)/\sigma^2}. \tag{20}$$

It was also shown that the distribution of distances closely resembles the Rician distribution, whose functional form depends on the ratio of $\|\mathbf{\Omega}_o\|/\sigma$. The distribution of distances may therefore be expressed as follows [1]:

$$\begin{aligned} f(\|\mathbf{\Omega}_r\|; \|\mathbf{\Omega}_o\|, \sigma) &= \int_0^{2\pi} f(\|\mathbf{\Omega}_r\|, \varphi)d\varphi \\ &= \frac{\|\mathbf{\Omega}_r\|}{2\pi\sigma^2} e^{-\left(\|\mathbf{\Omega}_r\|^2 + \|\mathbf{\Omega}_o\|^2\right)/2\sigma^2} \int_0^{2\pi} e^{\|\mathbf{\Omega}_r\|\|\mathbf{\Omega}_o\|\cos(\varphi-\varphi_o)/2\sigma^2}d\varphi \\ &= \frac{\|\mathbf{\Omega}_r\|}{\sigma^2} e^{-\left(\|\mathbf{\Omega}_o\|^2 + \|\mathbf{\Omega}_r\|^2\right)/2\sigma^2} \mathrm{I}_0\left(\frac{\|\mathbf{\Omega}_o\|\|\mathbf{\Omega}_r\|}{\sigma^2}\right), \|\mathbf{\Omega}_r\| \geq 0. \end{aligned} \tag{21}$$

In accordance with the above and after some simple algebraic manipulations, the conditional angular distribution takes the following form:

$$f(\varphi | \|\mathbf{\Omega}_r\|) = \frac{f_{R,\Phi}(\|\mathbf{\Omega}_r\|, \varphi)}{f(\|\mathbf{\Omega}_r\|; \|\mathbf{\Omega}_o\|, \sigma)} = e^{\|\mathbf{\Omega}_r\|\|\mathbf{\Omega}_o\|\cos(\varphi-\varphi_o)/\sigma^2}/2\pi\mathrm{I}_0\left(\frac{\|\mathbf{\Omega}_o\|\|\mathbf{\Omega}_r\|}{\sigma^2}\right). \tag{22}$$

Formulae (22) is another form of the von-Mises distribution, with the ratio $\|\mathbf{\Omega}_r\|\|\mathbf{\Omega}_o\|/\sigma^2$ being equivalent to the well-known concentration parameter κ. Conditioning the above to solely one distance (circumference of circle), translates to $\kappa = \|\mathbf{\Omega}_o\|^2/\sigma^2$. Restricting the value of $\|\mathbf{\Omega}_o\|$ to lie on the unit circle results in the

classic formulae that relates angular concentration and standard deviation, i.e. $\sigma = 1/\sqrt{\kappa}$. To counteract the loss of the radial dimension, the parameter κ should be divided by $\|\Omega_o\|^2$ in order to capture the effect of increased concentration due to changes in the mean directional vector.

VII. APPENDIX: FOURIER COEFFICIENTS

Any 2-D function $f(\varrho_r, \varphi_k)$ defined on the whole space can be expanded with respect to the Normal Fourier basis function, i.e. $\Psi = e^{-in\varphi_k}$. This signifies that a function is expandable in a series of cylindrical functions, the so-called cylindrical harmonics, that need not necessarily be of unit length. In mathematical terms this translates to:

$$f(\varrho_r, \varphi_k) = \int_0^\infty \sum_{n=-\infty}^\infty \delta(\varrho_r) e^{-in\varphi_k} \varrho_r d\varrho_r. \tag{23}$$

The coefficients of the Fourier transform become a function of ϱ_r and may be directly obtained from:

$$\delta(\varrho_r) = \int_0^\infty \int_0^{2\pi} f(\varrho_r, \varphi_k) e^{-in\varphi_k} \varrho_r d\varrho_r d\varphi_k = \underbrace{\int_0^\infty f(\varrho_r) \varrho_r d\varrho_r}_{\text{First-order moment of I-G Power Density}} \underbrace{\int_0^{2\pi} f(\varphi_k) e^{-in\varphi_k} d\varphi_k}_{\text{Characteristic Function of Angular Density}}.$$
$$\tag{24}$$

The coefficients are formed by the product of the expected power of the Inverse-Gamma distribution and the *characteristic function* of the angular density function in (2). The first-order moment of an I-G distributed random variable, P_r, is given by:

$$E[P_r] = \frac{\beta^\alpha}{\Gamma[\alpha]} \beta^{1-\alpha} \Gamma[\alpha - 1] = \frac{\beta}{\alpha - 1}. \tag{25}$$

The situation is more complicated for the integral involving the angular density function. To proceed, (2) should be simplified in order to succeed in obtaining an analytical expression for the integral in consideration. It was found that the von-Mises density provides a good approximation of the angular density in (2), at least for $\|\Omega_o\| \geq 2\sigma$. The degree of approximation in case the length of the mean directional vector Ω_o is greater than 2σ follows a similar reasoning as the one attributed to the symmetrical and asymmetrical regions of the distance distribution, explained in [1]. However, the parameters of the original density are lost by this approximation, and is left purely to the parameters of the von-Mises density to characterize any changes in distance. The proof of this relationship was given earlier in Appendix VI. Proceeding with the approximation and using (9.6.19) in [22], we have:

$$\gamma_n = \int_0^{2\pi} f(\varphi_k) e^{-in\varphi_k} d\varphi_k = e^{in\varphi_o} \frac{I_n(\kappa)}{I_0(\kappa)}. \tag{26}$$

Thus, the coefficients take the following form:

$$\delta = E[P_r]\gamma_n = \frac{\beta}{\alpha - 1} e^{in\varphi_o} \frac{I_n(\kappa)}{I_0(\kappa)}. \tag{27}$$

REFERENCES

[1] K. Mammasis and P. Santi, "A Two-dimensional geometry-based stochastic model," *IEEE Trans. Wireless Commun.*, vol. 11, no. 1, pp. 38–43, 2012.

[2] 3GPP-SCM, "Spatial channel model for multiple input multiple output (MIMO) simulations. tr.25.966 v.6.10," *http://www.3gpp.org/.*, Sep. 2003.

[3] P. Kysti, J. Meinil, and et al., "WINNER II Channel Models, D1.1.2 v1.1, IST-4-027756," *http://www.ist-winner.org/*, Aug. 2007.

[4] K. I. Pedersen, P. E. Mogensen, and B. H. Fleury, "A stochastic model of the temporal and azimuthal dispersion seen at the base station in outdoor propagation environments," *IEEE Trans. Veh. Technol.*, vol. 49, no. 2, pp. 437–447, Mar. 2000.

[5] Q. H. Spencer, B. D. Jeffs, M. A. Jensen, and A. L. Swindlehurst, "Modeling the statistical time and angle of arrival characteristics of an indoor multipath channel," *IEEE J. Sel. Areas Commun.*, vol. 18, no. 3, pp. 347–360, Mar. 2000.

[6] R. Janaswamy, "Angle and time of arrival statistics for the Gaussian scatter density model," *IEEE Trans. Wireless Commun.*, vol. 1, no. 3, pp. 488–497, Jul. 2002.

[7] R. B. Ertel and J. H. Reed, "Angle and time of arrival statistics for circular and elliptical scattering models," *IEEE J. Sel. Areas Commun.*, vol. 17, no. 11, pp. 1829–1840, Nov. 1999.

[8] A. F. Molisch, "A generic model for MIMO wireless propagation channels in macro- and microcells," *IEEE Trans. Signal Process.*, vol. 52, no. 1, pp. 61–71, 2004.

[9] J. Fuhl, A. F. Molisch, and E. Bonek, "Unified channel model for mobile radio systems with smart antennas," *IEE Proceedings -Radar, Sonar and Navigation*, vol. 145, no. 1, pp. 32–41, Feb. 1998.

[10] F. Adachi, M. Feeny, W. A. Williamson, and J. Parsons, "Crosscorrelation between the envelopes of 900 MHz signals received at a mobile radio base station site," *IEE Proceedings Communications, Radar and Signal Processing*, vol. 133, no. 6, pp. 506–512, Oct. 1986.

[11] J. B. Andersen and K. I. Pedersen, "Angle-of-arrival statistics for low resolution antennas," *IEEE Trans. Antennas Propag.*, vol. 50, no. 3, pp. 391–395, Mar. 2002.

[12] T. M. Cover and J. A. Thomas, *Elements of Information Theory*, 2nd ed. John Wiley & Sons, 2006.

[13] K. I. Pedersen, P. E. Mogensen, and B. H. Fleury, "Spatial channel characteristics in outdoor environments and their impact on BS antenna system performance," in *Proc. 48th IEEE Veh. Technol. Conf. (VTC 98)*, vol. 2, 18–21 May 1998, pp. 719–723.

[14] K. Kalliola, H. Laitinen, P. Vainikainen, M. Toeltsch, J. Laurila, and E. Bonek, "3-D double-directional radio channel characterization for urban macrocellular applications," *IEEE Trans. Antennas Propag.*, vol. 51, no. 11, pp. 3122–3133, Nov. 2003.

[15] A. F. Molisch, "Effect of far scatterer clusters in MIMO outdoor channel models," in *Proc. Veh. Technol. Conf., (VTC 2003-Spring)*, vol. 1, 22-25 Apr. 2003, pp. 534–538.

[16] N. Czink, P. Cera, J. Salo, E. Bonek, J.-P. Nuutinen, and J. Ylitalo, "A framework for automatic clustering of parametric MIMO channel data including path powers," in *Proc. VTC-2006 Fall Vehicular Technology Conf. 2006 IEEE 64th*, 2006, pp. 1–5.

[17] K. Mammasis and R. W. Stewart, "Spatial fading correlation model using mixtures of vMF distributions," *IEEE Trans. Wireless Commun.*, vol. 8, no. 4, pp. 2046 – 2055, Apr. 2009.

[18] S. K. Yong and J. S. Thompson, "Three-dimensional spatial fading correlation models for compact MIMO receivers," *IEEE Trans. Wirel. Commun.*, vol. 4, no. 6, pp. 2856–2869, Nov. 2005.

[19] P. D. Teal, T. D. Abhayapala, and R. A. Kennedy, "Spatial correlation for general distributions of scatterers," *IEEE Signal Process. Lett.*, vol. 9, no. 10, pp. 305–308, Oct. 2002.

[20] W. C. Jakes, *Microwave Mobile Communications*. New York: John Wiley & Sons, 1974.

[21] D. ManhTuan, N. Viet-Anh, and S.-O. Park, "Derivation and analysis of spatial correlation for 2x2 mimo system," *IEEE Antennas Wireless Propag. Lett.*, vol. 8, pp. 409–413, 2009.

[22] M. Abramowitz and I. A. Stegun, *Handbook of Mathematical Functions*, Dover, 1964.

[23] A. Goldsmith, *Wireless Communications*. Cambridge University Press, 2005.
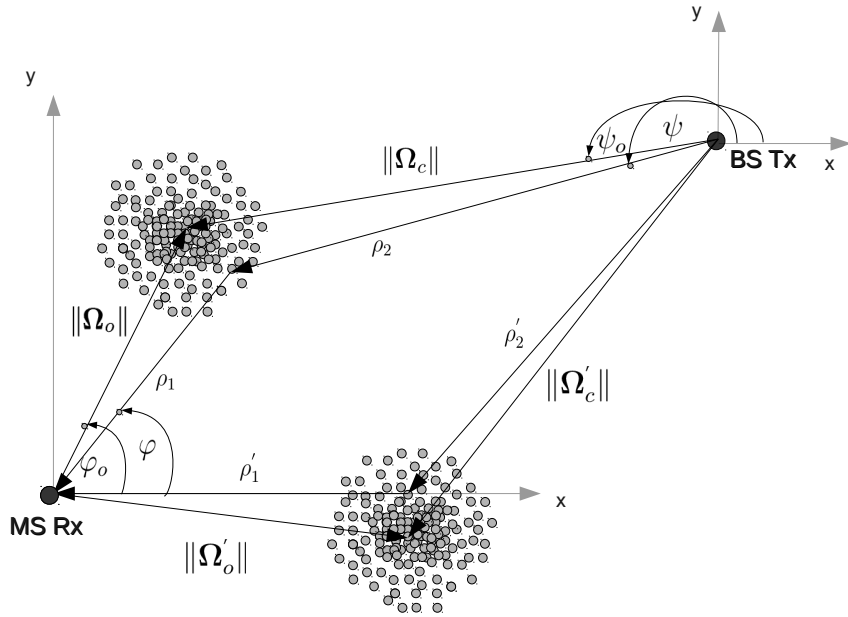
Fig. 1: This figure presents the geometrical structure of a two-cluster channel topology.
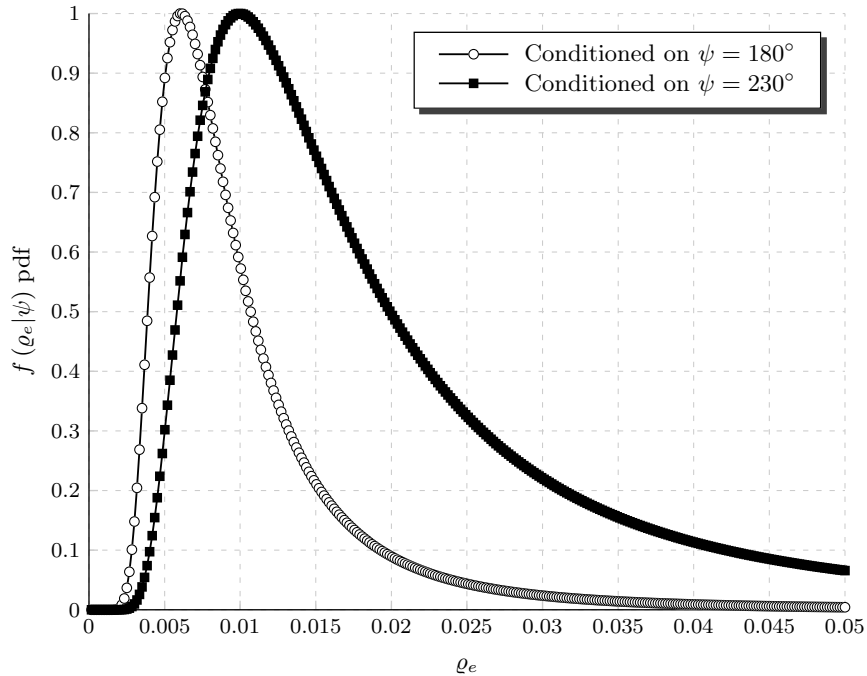

Fig. 2: This figure illustrates the effect of altering the angle at which the power distribution is conditioned for a constant set of parameters Ω_o, σ, ψ_o on the derived power conditional density function. Note that a direct comparison between the expected conditional values of the two curves does not lead to intuitive results since both should be scaled by the probability density in angle of arrival.
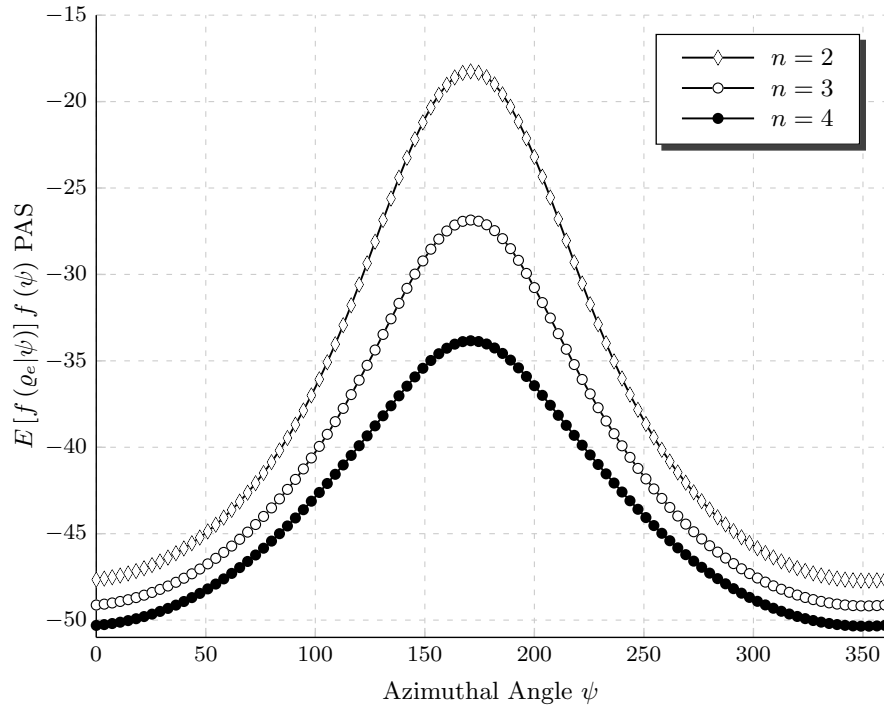
Fig. 3: Estimated PAS in accordance with (9) for various path-loss exponents. To focus on the impact that higher path-loss exponents exhibit on the power angular profile, i.e. PAS, the *y*-axis has been logarithmically scaled [dB]. The derived PAS seems to follow a Gaussian distribution for the free-space path loss exponent, while it more accurately approximates a heavily tailed function, e.g. Lorentzian, as the exponent increases. To place an upper limit on the original power conditional distribution and thus obtain the truncated conditional density, $f(\varrho_e|\varphi)$ has been truncated at 10% of the length of the mean directional vector. This places the boundary of the far-field zone at $r_{min} = 1$, corresponding to a frequency f in the MHz range.
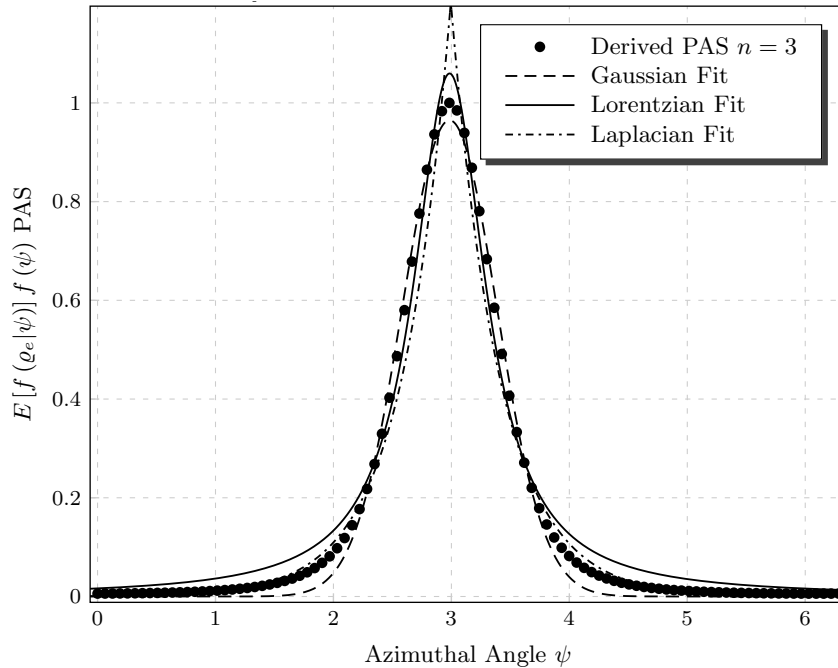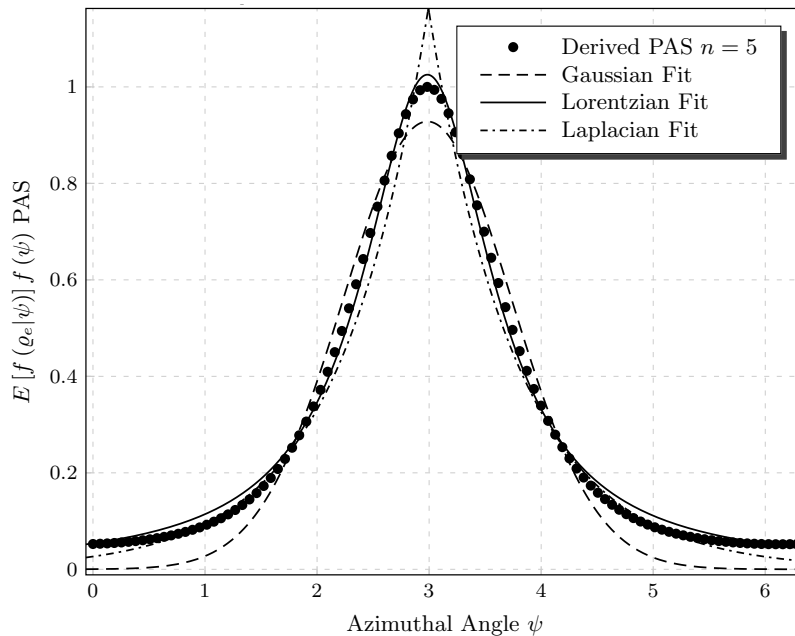
(a) Model assessement for path-loss exponent $n = 3$.

(b) Model assessement for path-loss exponent $n = 5$.

Fig. 4: This figure illustrates a comparison between the estimated normalized PAS for $n = 3$ and $n = 5$, and the corresponding Lorentzian, Laplacian and Gaussian fits in linear scale. The x-axis is scaled in radians. As shown, the Lorentzian function provides an excellent fit with an estimated scale parameter in the order of 1.8. In fact the computed mean square error indicated that the Lorentzian function outperforms all other candidate models for both $n = 3$, $n = 4$ and $n = 5$ types of exponents. Path-loss exponents in the range of $n = 3$ are typical in urban micro type of cells, while path-loss exponents $n > 3.7$ typically characterize urban macrocells [23]. Note that as the path-loss exponent increases the tails of the PAS extend further.
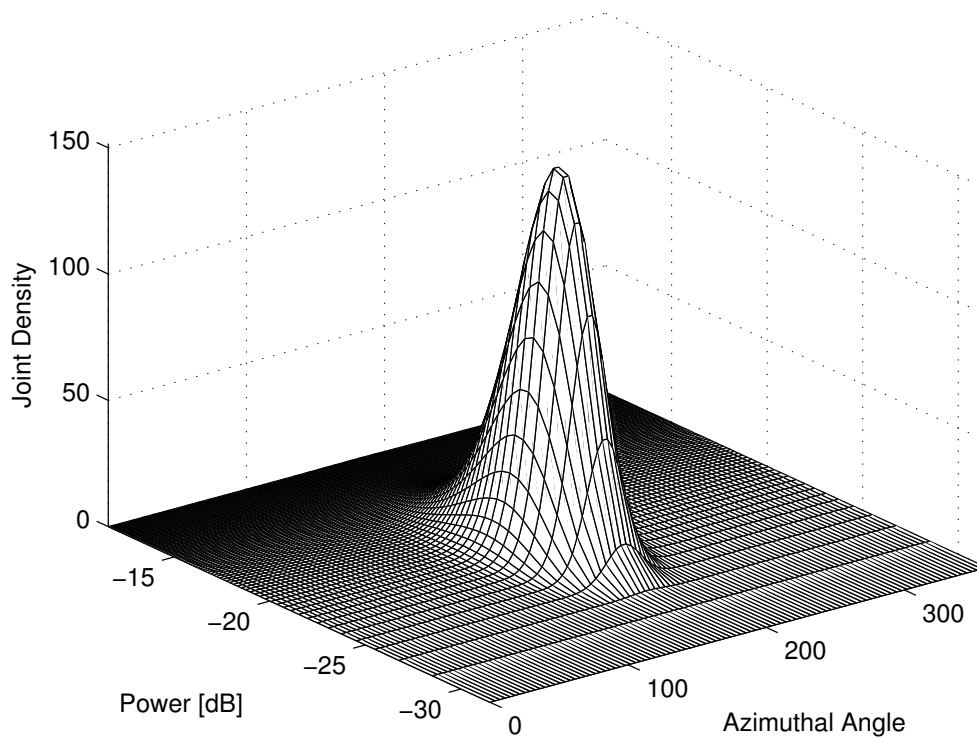
Fig. 5: The transmitting power angular scattering response is shown for the exemplary case of $\|\mathbf{\Omega}_o\| = 10$, $\sigma = 3$ and $\psi_o = 180^o$. The response is plotted against power ϱ_e (dB-scale) and the azimuthal angle ψ.
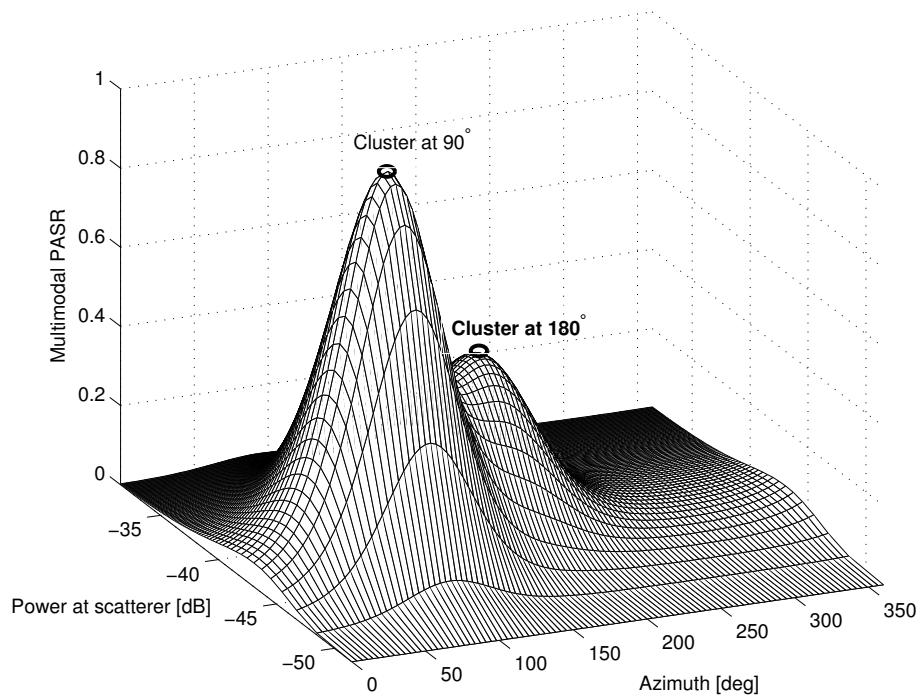
Fig. 6: Estimated multimodal PASR for two clusters located at $\varphi_o = 90°$ and $\varphi_o = 180°$ respectively. The derived modeling approach captures the effect of increased distance due to the second cluster, i.e. $\Omega'_c = 16$, and reflects it on the PASR by assigning a lower power weight on the second lobe at $\varphi_o = 180°$.
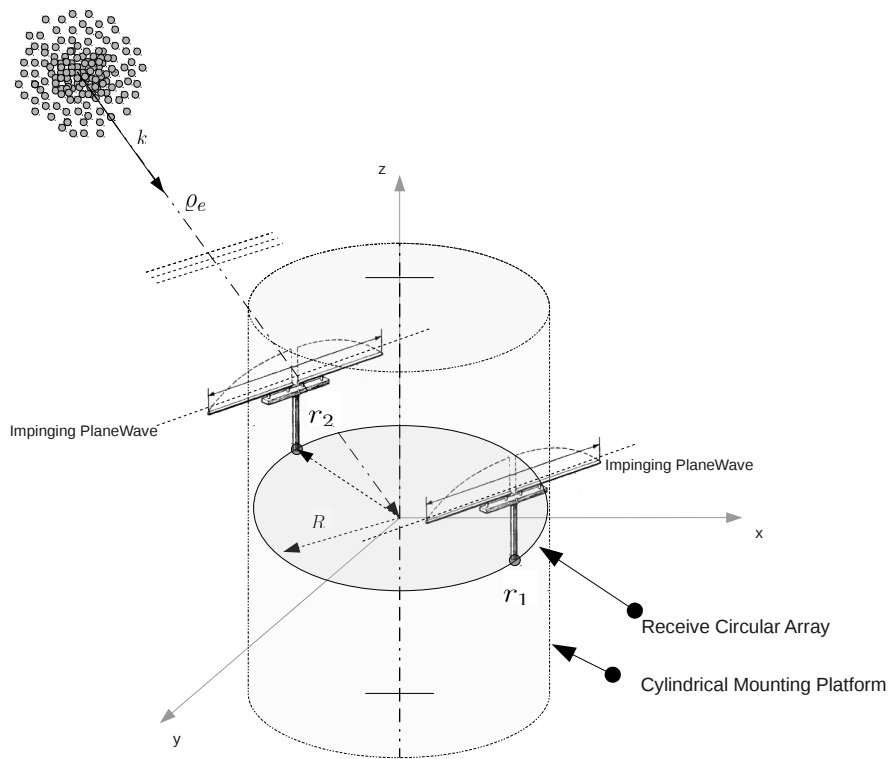
Fig. 7: A series of plane waves originated from a distant cluster, impinge on a circular array of radius R. Two horizantally oriented dipoles are present in the array, on position r_1 and r_2 respectively. The plane waves are characterized by the wavevector k, whose associated angle is ϑ, φ. Observe that in practical implementations the dipole elements are vertically oriented. The array is mounted on a cylindrical platform.
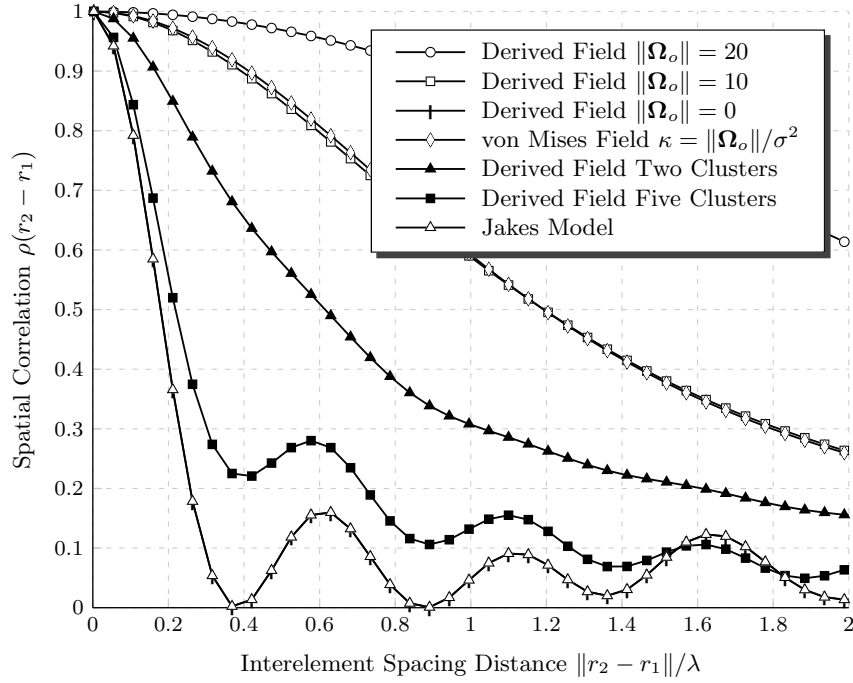
Fig. 8: Correlation estimates between antenna patterns for different impinging fields and various inter-element spacings. These estimates were computed for various lengths of the mean directional vector. For the multimodal two cluster case depicted also on the same figure the parameters are as detailed in Section IV.
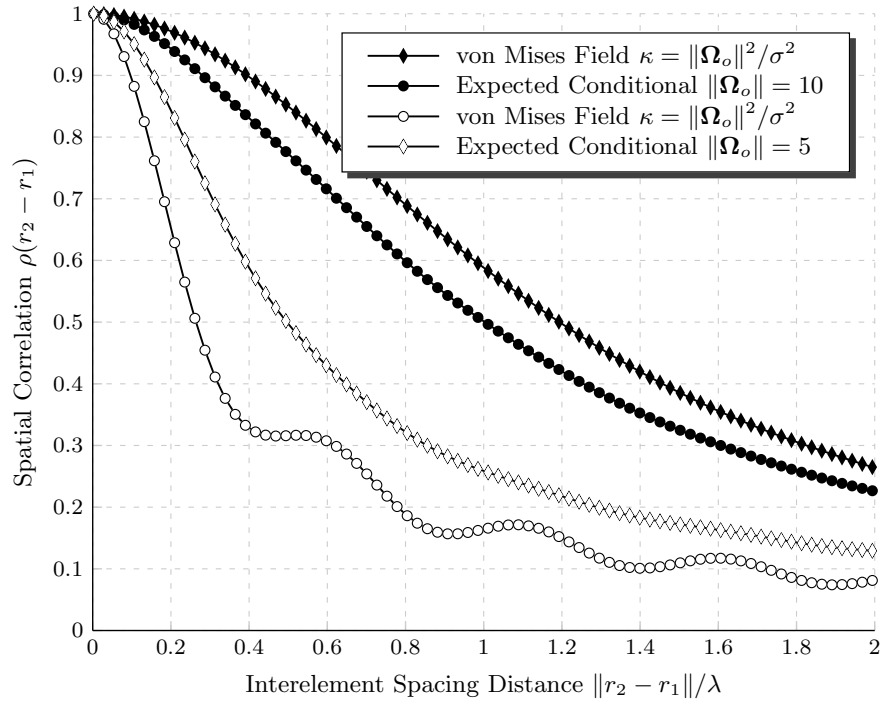

Fig. 9: Correlation estimates between antenna patterns for estimated PAS and various inter-element spacings reveals the resultant over-estimation of the von-Mises model. Two different cases are drawn: $\|\mathbf{\Omega}_o\| = 10$ and $\|\mathbf{\Omega}_o\| = 5$.

TABLE I: Parameter estimates of the power density function for various lengths of the mean distance vectors and $\sigma = 3$.

$\|\mathbf{\Omega}_o\|$ or $\|\mathbf{\Omega}_c\|$	α	β
1	1.2648	0.0632
2	1.2527	0.0545
3	1.3056	0.0418
4	1.3411	0.0386
5	1.5887	0.0359
6	1.8764	0.0339
7	2.2971	0.0334
8	2.6421	0.0316
9	3.0233	0.0302
10	3.7346	0.0311
12	4.6736	0.0287
14	5.9937	0.0279
16	7.7332	0.0281
20	11.814	0.0282
25	17.771	0.0276
30	25.381	0.0276
35	34.572	0.0277
40	45.075	0.0278

TABLE II: List of Derived Distributions and Associated Approximations.

Derived Distributions	Approximations Performed
$f(\psi; \|\mathbf{\Omega}_o\|, \sigma)$	The derived angular distribution remains unchanged throughout the paper. Nonetheless, the distribution can be approximated by a von-Mises distribution in case $\|\mathbf{\Omega}_o\| \geq 2\sigma$.
$f(\|\mathbf{\Omega}_{\rho_2,sc}\| \| \psi)$	The derived conditional distance density also remains unchanged in this work.
$f(\varrho_e \| \psi)$	This distribution expresses the conditional power density in each angle and is a key function for the analysis presented herein. It is well approximated using the Inverse-Gamma distribution.
$f(\varrho_e, \psi)$	The joint distribution of power and angle defining the so-called *power angular scattering response*.
$f(\varrho_r \| \varphi)$	The conditional distribution at the TX-BS is derived by using the appropriate transformation function, resulting in the product of two Inverse-Gamma random variables. The first random variable is due to $f(\varrho_e \| \psi)$ and the second arises directly from the new set of distances between the TX-BS and the scatter cluster, which has exactly the same distribution (detailed analysis in Section II-B). Therefore, $f(\varrho_r \| \varphi)$ is a scaled version of $f(\varrho_e \| \psi)$.
$f(\varrho_e)$	If the assumption of independence between the radial and the angular domain is claimed, then as shown in [1], $f(\varrho_e)$ may be well approximated using the Inverse-Gamma distribution.
$f(\varrho_r)$	Similarly, and by using the transformation function presented therein, the power density at the receiver resulting from the product of two Inverse-Gamma random variables can also be approximated by an Inverse Gamma distribution.